

Automatika

Journal for Control, Measurement, Electronics, Computing and Communications

ISSN: (Print) (Online) Journal homepage: www.tandfonline.com/journals/taut20

Set-based fast gradient projection algorithm for model predictive control of grid-tied power converters

Renato Babojelić, Bruno Vilić Belina, Šandor Ileš & Jadranko Matuško

To cite this article: Renato Babojelić, Bruno Vilić Belina, Šandor Ileš & Jadranko Matuško (2023) Set-based fast gradient projection algorithm for model predictive control of grid-tied power converters, *Automatika*, 64:2, 304-314, DOI: [10.1080/00051144.2022.2149062](https://doi.org/10.1080/00051144.2022.2149062)

To link to this article: <https://doi.org/10.1080/00051144.2022.2149062>



© 2022 The Author(s). Published by Informa UK Limited, trading as Taylor & Francis Group.



Published online: 28 Nov 2022.



Submit your article to this journal [↗](#)



Article views: 578




View related articles [↗](#)



View Crossmark data [↗](#)



Set-based fast gradient projection algorithm for model predictive control of grid-tied power converters

Renato Babojelić, Bruno Vilić Belina, Šandor Ileš and Jadranko Matuško 

Faculty of Electrical Engineering and Computing, University of Zagreb, Zagreb, Croatia

ABSTRACT

Model Predictive Control (MPC) has attracted much attention and is widely used in power electronics. However, implementing the MPC algorithm is still a difficult task due to the fast dynamics of power converters and strict time constraints. In this paper, a computationally efficient MPC algorithm for grid-tied power converters based on the fast gradient projection method and invariant set theory is proposed. The algorithm is implemented and tested through hardware-in-the-loop simulations using Texas Instruments digital signal processors and Xilinx Field Programmable Gate Arrays platforms.

ARTICLE HISTORY

Received 15 May 2022

Accepted 14 November 2022

KEYWORDS

Power converters; model predictive control; robust control; fast gradient projection method; field programmable gate array

1. Introduction

In recent years, the use of Model predictive control (MPC) in power electronics applications has seen an increased use, mainly owing to the increase in computing power and the inception of powerful embedded devices [1–3]. Two distinct approaches to model predictive control of power converters are seen in the literature, the finite control set (FCS-MPC) and the continuous control set (CCS-MPC). Due to their switching nature, power converters possess a finite number of control vectors; this, in combination with short prediction horizons of length one or two, allows FCS-MPC algorithms to simply check all the switching states to find the optimal one, which is then directly applied to the power converter's switches. Predictive controllers using CCS-MPC need to solve an optimization problem at each sampling time and output the optimal continuous control vector that is then applied to the power converter using a modulator.

The use of the FCS-MPC approach allows for simple and fast optimization algorithms but requires additional care in controller design to ensure stability, since the control signal is always selected from the finite control set [4–6]. In addition, an extension of the control horizon has also been considered, but this may lead to intractable optimization problems requiring advanced optimization algorithms [7,8].

By overlooking the discrete nature of the power converter, the CCS-MPC allows for longer prediction horizons, and the constant switching frequency also

provides an additional advantage to the CCS-MPC [9]. This fact is especially important for power converters using LCL filters, as the filters are designed for particular switching frequencies [10].

The main challenge in implementing controllers that use either approach is meeting the strict execution time constraints imposed by the fast dynamics of power converters. Recently, significant progress has been made in the area of numerically efficient predictive control algorithms, and intensive research continues in this area in both academia and industry. One of the simplest and most widely used approaches to efficiently solving finite-horizon optimal control problems is based on the well-known fast (accelerated) gradient projection method (FGM), first introduced by Nesterov in 1983 [11]. However, the FGM algorithm can only be used for MPC problems with input constraints where the set of input constraints is relatively simple and allows efficient projection of the candidate solution onto the set of input constraints. Several solutions have been proposed to enable FGM to handle state constraints as well. Among them, a dual FGM has attracted the most interest.

The use of FGM in the control of power converters can be found in the literature for applications such as controlling the grid-tied rectifier [11] or driving the permanent magnet synchronous machine [12]. Both approaches use standard quadratic-cost MPC with only input constraints, with the former approach requiring the use of horizons of length three or more, owing to the higher-order LCL filter.

In the literature, embedded devices used to control power converters are mainly Digital signal processors (DSP) and Field Programmable Gate Arrays (FPGA). Due to its inherent parallelism, FPGA is the most promising solution for implementing MPC. Traditionally used as hardware interface logic circuits, they have seen a dramatic price reduction over the past decade while increasing the density of logic elements on a chip. In addition, FPGAs offer advantages over micro-controllers or DSPs in power converter applications by reducing computation time, resulting in lower control delay and better dynamic performance [13].

This paper presents a set-based fast gradient approach to control of grid-tied power converters with an LCL filter and proposes an efficient implementation of a set-based MPC algorithm using the modified fast gradient projection method for solving the optimization problem. The need for use of the Dual FGM to handle state constraints in the optimization problem is here circumvented by transforming the state constraints to input constraints using invariant sets theory; as the input constraints are ellipsoidal sets they allow for an efficient projection operation in the FGM. The proposed control approach, which is based on a sequence of one-step control invariant sets, also provides an explicit guarantee of closed-loop stability without introducing the additional conservatism found in MPC controllers with guaranteed stability. Furthermore, by extending this approach to linear parameter varying (LPV) systems, the MPC algorithm is made robust to the uncertainties in the variation of the grid inductance. The proposed approach was tested in hardware-in-the-loop simulation.

The paper is divided into sections as follows: Section 2 introduces the mathematical model of a grid-tied two-level inverter with an LCL filter; Section 3 presents a set-based model predictive control algorithm; and Section 4 presents a modified fast gradient method for solving the MPC optimization problem. Section 5 describes the LPV model and needed modifications to the MPC algorithm to allow for the robust handling of variation in grid inductance, and Section 6 describes the offline precomputation of data needed for implementation in embedded systems. Section 7 shows the simulation results of a proposed algorithm, and Section 8 concludes the paper.

2. Mathematical model of a grid-tied inverter with an LCL filter

For a two-level, grid-tied, three-phase inverter with an LCL filter shown in Figure 1, define vectors $i_1 = [i_{1a} \ i_{1b} \ i_{1c}]^T$, $v_c = [v_{ca} \ v_{cb} \ v_{cc}]^T$, $i_2 = [i_{2a} \ i_{2b} \ i_{2c}]^T$ that represent three-phase quantities of inverter side currents, capacitor voltages, and grid side currents, respectively.

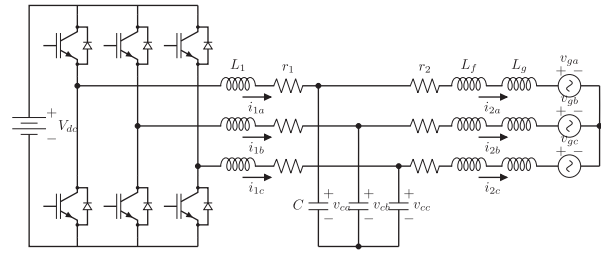


Figure 1. Two-level grid-tied inverter with an LCL filter.

Using Park's transformation

$$T_{dq}(\theta) = \frac{2}{3} \begin{bmatrix} \sin \theta & \sin \left(\theta - \frac{2}{3}\pi \right) & \sin \left(\theta + \frac{2}{3}\pi \right) \\ \cos \theta & \cos \left(\theta - \frac{2}{3}\pi \right) & \cos \left(\theta + \frac{2}{3}\pi \right) \end{bmatrix} \quad (1)$$

three-phase quantities are written in the dq rotating reference frame as

$$\begin{bmatrix} z_d \\ z_q \end{bmatrix} = T_{dq}(\theta) \begin{bmatrix} z_a \\ z_b \\ z_c \end{bmatrix} \quad (2)$$

where $z \in \{i_1, v_c, i_2, v_g\}$.

Define $x(t) = [i_{1d}(t) \ i_{1q}(t) \ v_d(t) \ v_q(t) \ i_{2d}(t) \ i_{2q}(t)]^T$ as the state vector with quantities in rotating reference frame, voltages applied by the inverter as vector $u(t) = [u_d(t) \ u_q(t)]^T$ and the grid voltages as $v(t) = [v_{gd}(t) \ v_{gq}(t)]^T$. The grid injected currents represent the systems controlled output $y(t) = [i_{2d}(t) \ i_{2q}(t)]^T$. From this, the linear state-space model in continuous time is written as

$$\begin{aligned} \dot{x}(t) &= Ax(t) + Bu(t) + Dv(t) \\ y(t) &= Cx(t) \end{aligned} \quad (3)$$

with system matrices defined as

$$A = \begin{bmatrix} -\frac{r_1}{L_1} & \omega & -\frac{1}{L_1} & 0 & 0 & 0 \\ -\omega & -\frac{r_1}{L_1} & 0 & -\frac{1}{L_1} & 0 & 0 \\ \frac{1}{C} & 0 & 0 & \omega & -\frac{1}{C} & 0 \\ 0 & \frac{1}{C} & -\omega & 0 & 0 & -\frac{1}{C} \\ 0 & 0 & \frac{1}{L_2} & 0 & -\frac{r_2}{L_2} & \omega \\ 0 & 0 & 0 & \frac{1}{L_2} & -\omega & -\frac{r_2}{L_2} \end{bmatrix},$$

$$B = \begin{bmatrix} 1/L_1 & 0 \\ 0 & 1/L_1 \\ 0 & 0 \\ 0 & 0 \\ 0 & 0 \\ 0 & 0 \end{bmatrix}, \quad D = \begin{bmatrix} 0 & 0 \\ 0 & 0 \\ 0 & 0 \\ 0 & 0 \\ -1/L_2 & 0 \\ 0 & -1/L_2 \end{bmatrix},$$

and

$$C = \begin{bmatrix} 0 & 0 & 0 & 0 & 1 & 0 \\ 0 & 0 & 0 & 0 & 0 & 1 \end{bmatrix},$$

where $\omega = 2\pi f$, with f denoting the grid frequency. Grid side inductance L_2 is comprised of filter inductance L_f , and grid inductance L_g (here assumed known and constant), i.e.

$$L_2 = L_f + L_g. \quad (4)$$

To obtain the discrete-time representation of the system with a constant sampling rate T_s the forward Euler approximation is used, which gives

$$\begin{aligned} x(k+1) &= A_d x(k) + B_d u(k) + D_d v(k) \\ y(k) &= C_d x(k) \end{aligned} \quad (5)$$

with

$$\begin{aligned} A_d &= I + T_s A, \\ B_d &= T_s B, \\ D_d &= T_s D, \\ C_d &= C. \end{aligned}$$

3. Ellipsoidal set-based MPC

Let us first introduce some basic definitions.

Definition 3.1: Let $\mathcal{X} \subseteq \mathbb{R}^n$ be the set of admissible states of a discrete-time system

$$\begin{aligned} x(k+1) &= Ax(k) + Bu(k), \\ y(k) &= Cx(k) \end{aligned} \quad (6)$$

and \mathcal{U} the set of all admissible control inputs. Set $\mathcal{T} \subseteq \mathcal{X}$ is said to be *control invariant* for the system if for every $x(k) \in \mathcal{T}$ there exists $u(k) \in \mathcal{U}$ such that $x(k+1) \in \mathcal{T}$.

Definition 3.2: For a system (6) define an *pre-set* of a set \mathcal{S} as

$$\Omega(\mathcal{S}) = \{x(k) \in \mathbb{R}^n \mid \exists u(k) \in \mathcal{U}, x(k+1) \in \mathcal{S}\}. \quad (7)$$

For a given set \mathcal{T} for a system (6) a sequence $\{\mathcal{T}_n\}_n$ of *one-step controllable sets* is defined by the following recursion

$$\begin{aligned} \mathcal{T}_0 &= \mathcal{T} \\ \mathcal{T}_n &= \Omega(\mathcal{T}_{n-1}) \cap \mathcal{X}. \end{aligned} \quad (8)$$

That is to say that every set in a sequence of sets $\{\mathcal{T}_n\}_{n \in \mathbb{N}}$ contains the states that can be steered to \mathcal{T}_{n-1} using a single control action.

As the exact sets $\{\mathcal{T}_n\}_{n \in \mathbb{N}}$ may be prohibitively complex for real-time use, *inner approximations* of these sets

are of interest. This leads to the following recursion, with \mathcal{T} control invariant for a system (6),

$$\begin{aligned} \tilde{\mathcal{T}}_0 &= \mathcal{T} \\ \tilde{\mathcal{T}}_n &= \mathbf{In} \left(\Omega(\tilde{\mathcal{T}}_{n-1}) \cap \mathcal{X} \right), \end{aligned} \quad (9)$$

where \mathbf{In} denotes the operation of finding an interior approximation of a given set (according to some predefined criterion).

In this paper, ellipsoidal inner approximations of such sets are used.

Definition 3.3: Let $P \in \mathbb{R}^{n \times n}$ be a symmetric positive (semi)definite matrix. *Ellipsoidal set* \mathcal{E}_P generated by matrix P , and centred at the origin, is defined as

$$\mathcal{E}_P = \{x \in \mathbb{R}^n \mid x^\top P x \leq 1\}. \quad (10)$$

If the generating matrix P is positive semidefinite it is said that the ellipsoid is *degenerate*.

Note that the degenerate ellipsoids have non-empty interiors and are unbounded in the directions of some of their semi-axes.

To compute the ellipsoidal approximations of the sequence of controllable sets, a computational scheme proposed in [14] is adopted. For a given stabilizing feedback matrix K for a system (6), and a non-empty invariant ellipsoid \mathcal{E} for a system $x(k+1) = (A + BK)x(k)$, assuming the input constraints satisfied in the ellipsoid \mathcal{E} , i.e. $\{Kx \mid x \in \mathcal{E}\} \subseteq \mathcal{U}$, the sequence of ellipsoidal sets is defined as

$$\begin{aligned} \mathcal{E}_0 &= \mathcal{E} \\ \mathcal{E}_n &= \mathbf{In} \left(\Omega(\mathcal{E}_{n-1}) \cap \mathcal{X} \right) \\ &= \mathbf{In} \left(\{x \in \mathbb{R}^n \mid \exists u \in \mathcal{U}, Ax + Bu \in \mathcal{E}_{n-1}\} \right) \cap \mathcal{X}. \end{aligned} \quad (11)$$

Note that the sequence obviously satisfies $\mathcal{E}_n \subseteq \mathcal{T}_n, \forall n$.

To obtain stabilizing feedback K for the system (6) the LMI (linear matrix inequality) [15] approach is adopted. To guarantee the closed-loop system stability, poles of a system situated inside of a circle with a radius r and centred at d , and the H_∞ cost of μ the following LMI feasibility problem is solved

$$\begin{bmatrix} P + P^\top - S & * & * \\ \frac{1}{r}(A - I)P + \frac{1}{r}BR & S & * \\ CP & 0 & \mu I \end{bmatrix} > 0. \quad (12)$$

Matrices $P, S \in \mathbb{R}^{n \times n}$ and $R \in \mathbb{R}^{m \times m}$ are symmetric positive definite, with $*$ denoting appropriate transposed blocks of blocks under the main diagonal. Stabilizing feedback gain is computed as

$$K = RP^{-1}. \quad (13)$$

For proof see [16].

From the stabilizing feedback gain K and the positive definite matrix P computed by (12) the final ellipsoidal set \mathcal{E}_0 is obtained by defining its generating matrix P_0 as

$$P_0 = \frac{\gamma}{u_{\max}^2} P, \quad (14)$$

where $u_{\max} \in \mathcal{U}$ is the vector with the maximum magnitude of an applicable control signal, and γ is a scaling factor computed by solving the optimization problem

$$\begin{aligned} \min_{\gamma \in \mathbb{R}} \quad & \gamma \\ \text{s.t.} \quad & K^\top K - \gamma P \leq 0, \\ & \gamma \geq 0. \end{aligned} \quad (15)$$

To construct the ellipsoids \mathcal{E}_n , $n \in \{1, \dots, m\}$ the procedure outlined in [14] is used.

Definition 3.4: Let the space $\mathbb{R}^n \times \mathbb{R}^m$ denote the *extended space* of all system states and all control inputs, where m is the dimension of the control input space. The ellipsoid in the extended space is the set

$$\tilde{\mathcal{E}}_{n-1} = \left\{ \begin{bmatrix} x \\ u \end{bmatrix} \in \mathbb{R}^n \times \mathbb{R}^m \mid Ax + Bu \in \mathcal{E}_{n-1} \right\}. \quad (16)$$

From Equation (11) and definition 3.4 it is easily shown that

$$\begin{aligned} \Omega(\mathcal{E}_{n-1}) &= \{x \in \mathbb{R}^n \mid \exists u \in \mathcal{U}, Ax + Bu \in \mathcal{E}_{n-1}\} \\ &\supseteq \mathbf{Proj}_x \left(\mathbf{In} \left(\tilde{\mathcal{E}}_{n-1} \cap (\mathbb{R}^n \times \mathcal{E}^{\mathcal{U}}) \cap \mathcal{E}^{\mathcal{X}} \right) \right) \\ &= \mathcal{E}_n, \end{aligned} \quad (17)$$

where \mathbf{Proj}_x is the projection operator from the extended space to the state space. The sets $\mathcal{E}^{\mathcal{U}}$ and $\mathcal{E}^{\mathcal{X}}$ represent the ellipsoids or possibly the intersection of ellipsoids representing the input and state constraints, respectively.

To calculate the set $\tilde{\mathcal{E}}_{n-1}$ in the extended space as defined in Definition 3.4, let P_{n-1} be the positive definite matrix defining the set \mathcal{E}_{n-1} in the state space, let also families of positive definite matrices $P_{\mathcal{U},i}$, $P_{\mathcal{X},i}$ represent the ellipsoidal sets that in intersection give $\mathcal{E}^{\mathcal{U}}$ and $\mathcal{E}^{\mathcal{X}}$. From Equations (10) and (16), it follows that $[x^\top u^\top]^\top \in \tilde{\mathcal{E}}_{n-1}$ if and only if

$$Ax + Bu \in \mathcal{E}_{n-1} \iff (18)$$

$$(Ax + Bu)^\top P_{n-1} (Ax + Bu) \leq 1 \iff (19)$$

$$\begin{bmatrix} x \\ u \end{bmatrix}^\top \begin{bmatrix} A^\top P_{n-1} A & A^\top P_{n-1} B \\ B^\top P_{n-1} A & B^\top P_{n-1} B \end{bmatrix} \begin{bmatrix} x \\ u \end{bmatrix} \leq 1, \quad (20)$$

and

$$u^\top P_{\mathcal{U},i} u \leq 1, \quad i \in \{1, \dots, n_{\mathcal{U}}\}, \quad (21)$$

$$x^\top P_{\mathcal{X},i} x \leq 1, \quad i \in \{1, \dots, n_{\mathcal{X}}\}. \quad (22)$$

The block matrix in Equation (20) represents the generating matrix of the wanted ellipsoid $\tilde{\mathcal{E}}_{n-1}$.

Let the positive definite matrix P represent the ellipsoidal set $\tilde{\mathcal{E}}_P$ in the extended space, it can be written in block matrix form as

$$P^{-1} = Q = \begin{bmatrix} Q_{11} & Q_{12} \\ Q_{12}^\top & Q_{22} \end{bmatrix} \quad (23)$$

The projection operation into the state space is given by

$$\begin{aligned} \mathbf{Proj}_x \left\{ \begin{bmatrix} x \\ u \end{bmatrix} \mid \begin{bmatrix} x \\ u \end{bmatrix}^\top \begin{bmatrix} Q_{11} & Q_{12} \\ Q_{12}^\top & Q_{22} \end{bmatrix}^{-1} \begin{bmatrix} x \\ u \end{bmatrix} \leq 1 \right\} \\ = \{x \mid x^\top Q_{11}^{-1} x \leq 1\}. \end{aligned} \quad (24)$$

To compute the interior approximation in Equation (17) of an intersection of k ellipsoids represented with positive definite matrices P_j the following LMI optimization problem to maximize the volume of the ellipsoid is posed

$$\begin{aligned} \max_{Q \geq 0} \quad & \log \det Q_{11} \\ \text{s.t.} \quad & 0 < \begin{bmatrix} Q_{11} & Q_{12} \\ Q_{12}^\top & Q_{22} \end{bmatrix} \leq P_j^{-1}, \quad j \in \{1, \dots, k\}. \end{aligned} \quad (25)$$

For the case of degenerate ellipsoids represented by positive semidefinite matrices P_j , as inverse P_j^{-1} is not defined, matrices can be decomposed as

$$P_j = U_j^\top \Lambda_j U_j \quad (26)$$

where U_j is an orthogonal matrix, and

$$\Lambda_j = \begin{bmatrix} \tilde{\Lambda}_j & 0 \\ 0 & 0 \end{bmatrix} \quad (27)$$

with $\tilde{\Lambda}_j$ diagonal. Geometrically, non-zero diagonal members in a matrix Λ_j represent all the bounded directions of ellipsoid's semi-axes, while the zeros on the diagonal represent unbounded directions. The optimization problem (25) can then be rewritten as

$$\begin{aligned} \max_{Q \geq 0} \quad & \log \det Q_{11} \\ \text{s.t.} \quad & 0 < \begin{bmatrix} I_j \\ 0 \end{bmatrix}^\top U_j \begin{bmatrix} Q_{11} & Q_{12} \\ Q_{12}^\top & Q_{22} \end{bmatrix} U_j^\top \begin{bmatrix} I_j \\ 0 \end{bmatrix} \leq \tilde{\Lambda}_j^{-1}, \\ & j \in \{1, \dots, k\}, \end{aligned} \quad (28)$$

where Q is the block matrix consisting of blocks Q_{11} , Q_{12} and Q_{22} , and I_j the identity matrix of appropriate dimensions.

Finally, iteratively solving the problem (28), matrices $P_n = Q_{11,n}^{-1}$ defining the ellipsoids \mathcal{E}_n are obtained. As mentioned, this procedure can be carried out offline to ease the computational burden, with the precomputed ellipsoidal sets then used in the real-time part of the algorithm. The real-time Set-based ellipsoidal MPC algorithm can now be formulated as Algorithm 1, with some appropriate cost function J .

Algorithm 1: Set-based Ellipsoidal MPC

Data: Discrete-time instance $k = 0$, state vector $x(k)$, precomputed ellipsoidal sets \mathcal{E}_n , system matrices A and B .

Start: Obtain measured state $x(k)$.

Find: $n(k) = \min\{n \mid x(k) \in \mathcal{E}_n\}$.

Solve:

$$\begin{aligned} u(k) &= \underset{u(k)}{\operatorname{argmin}} J(x(k), u(k)) \\ \text{s.t.} & \\ Ax(k) + Bu(k) &\in \mathcal{E}_{n(k)-1} \end{aligned} \quad (29)$$

$k = k + 1$

Result: Control action $u(k)$

Return to Start

At every time instance k , the MPC algorithm first finds the minimal index $n(k)$ of all ellipsoids \mathcal{E}_n that contain the state vector $x(k)$; after that, the optimization problem (29) is solved to find the control action $u(k)$ that steers the system state to the next ellipsoid, i.e. $x(k+1) \in \mathcal{E}_{n(k)-1}$.

4. Computationally efficient set-based MPC based on fast gradient projection method

As power inverters employ very fast system dynamics, with switching times in the kHz range, for real-time use of Algorithm 1, its implementation needs to run in the range of tens of microseconds. This section describes the modification of the fast gradient projection method (FGM) to efficiently solve the optimization problem (29) that is a crucial part of Algorithm 1.

The fast gradient projection method, originally proposed by Nesterov in 1983, instead of computing the Hessian matrix of a cost function, accelerates the standard gradient descent method by estimating the bounds on its second-order differential information. Furthermore, FGM is able to handle constraints on the optimization variable; to ensure the feasibility of a solution, the candidate solution is projected on the feasible set. As a downside, this increases the number of iterations needed to find the optimal solution. Also, for solving the MPC problem using FGM, one is limited to MPC problem formulations containing only the constraints on the control variable and not the state variable, and requiring the input constraint set to be relatively simple for the projection operation to be efficiently computed.

Let us assume the MPC problem in the standard form with a quadratic cost function

$$J_N^*(x) := \min \frac{1}{2} x_N^\top P x_N + \frac{1}{2} \sum_{k=0}^{N-1} x_k^\top Q x_k + u_k^\top R u_k$$

$$\text{s.t. } x_{k+1} = Ax_k + Bu_k, \quad \forall k = 0 \dots N-1$$

$$\begin{aligned} u_k &\in \mathcal{U}, \quad \forall k \in \{0, \dots, N-1\} \\ x_0 &= x. \end{aligned} \quad (30)$$

Rewriting J as a function of the initial state and inputs, a batch form of the problem is obtained

$$\begin{aligned} J_N^*(x) &= \min J_N(U; x) \\ \text{s.t. } &U \in \mathcal{U}^N. \end{aligned} \quad (31)$$

As the cost function $J_N(U; x)$ is quadratic, it is also strongly convex, and its gradient is Lipschitz continuous, which means that it can be upper- and lower-bounded. For this class of functions, the fast gradient method can be formulated as Algorithm 2. In the Algorithm 2 L represents the Lipschitz constant of the gradient of the objective function, $\mathbf{Proj}_{\mathcal{U}^N}$ represents the projection operator on the feasible set \mathcal{U}^N . While scalars β_i , $i \in \{0, \dots, i_{\max}-1\}$ represent the scaling factors that can be precomputed from the Lipschitz constant L and the convexity parameter μ . Parameter μ satisfies $\nabla^2 J_N(U; x) = 2H \geq \mu I$. That is, $\mu > 0$ is the under-approximation of the minimum eigenvalue of $2H$.

Algorithm 2:

 Fast gradient method for constrained minimization

Data: Initial point $u_0 \in \mathcal{U}^N$, $y_0 = u_0$, number of iterations i_{\max} , Lipschitz constant L , scaling factors $\beta_0, \dots, \beta_{i_{\max}-1}$

for $i = 0 \rightarrow i_{\max} - 1$ **do**

$$v_{i+1} = y_i - \frac{1}{L} \nabla J_N(y_i) = My_i + g;$$

$$U_{i+1} = \mathbf{Proj}_{\mathcal{U}^N}(v_{i+1});$$

$$y_{i+1} = U_{i+1} + \beta^i (U_{i+1} - U_i).$$

end

Result: Control sequence U .

Important part of FGM Algorithm 2 is the projection operation where a candidate solution v_{i+1} is projected onto input constraint set \mathcal{U}^N . In a case where input constraint set \mathcal{U}^N is simple (e.g., box constraints, circle), the projection operation can be performed very efficiently. In the following subsection, the FGM algorithm based on ellipsoidal sets is described.

4.1. Equilibrium point

For a given reference vector $r = [i_{dr} \ i_{qr}]^\top$, the equilibrium point $[x_d \ u_d]^\top$ of a system (3) is

$$\begin{bmatrix} x_d \\ u_d \end{bmatrix} = \begin{bmatrix} A & B \\ C & 0 \end{bmatrix}^{-1} \begin{bmatrix} -Dv \\ r \end{bmatrix}. \quad (32)$$

To obtain the error dynamics of a system (5) with known grid voltage v and for a chosen output reference r , define $e(k) = x(k) - x_d$ as an error around

equilibrium point $[x_d \ u_d]^\top$, which leads to

$$e(k+1) = A_d e(k) + B_d u_{\text{err}}(k), \quad (33)$$

where $u_{\text{err}}(k) = u(k) - u_d$.

4.2. Set-based fast gradient projection method

For controlling the system (33), the optimization problem (29) has to be solved in real time at every time step. The fact that the optimization problem contains constraints on the state-space variable, i.e., requiring that the state in the next time step belongs to the next ellipsoid until reaching the terminal ellipsoid, allows us to constrain our choice of cost functions to simpler one-step prediction formulations without sacrificing stability but also requires the modification of the problem by replacing the state constraints with corresponding input constraints

$$\begin{aligned} u_{\text{err}}(k) &= \underset{u_{\text{err}}}{\text{argmin}} J(u_{\text{err}}(k), e(k)) \\ \text{s.t. } u_{\text{err}}(k) &\in \mathcal{U}_k(e(k)) \end{aligned} \quad (34)$$

where the set $\mathcal{U}_k(e(k))$ is defined as

$$\mathcal{U}_k(e(k)) = \{u(k) \mid A_d e(k) + B_d u_{\text{err}}(k) \in \mathcal{E}_{n(k)-1}\}. \quad (35)$$

This means that for a given state $e(k)$ the set $\mathcal{U}_k(e(k))$ represents a set containing all control inputs that will steer the next state $e(k+1)$ to the set $\mathcal{E}_{n(k)-1}$. To obtain the set $\mathcal{U}_k(e(k))$, assume $e(k)$ in an ellipsoid \mathcal{E}_i , the set

$$\tilde{\mathcal{E}}_n = \mathbf{In} \left(\tilde{\mathcal{E}}_n \cap (\mathbb{R}^6 \times \mathcal{E}^u) \right) \quad (36)$$

is an ellipsoid in the extended space that contains the vector $[e(k) \ u(k)]^\top$. This implies that the set $\tilde{\mathcal{E}}_n$ is represented by a symmetric positive semidefinite matrix $\bar{P} \in \mathbb{R}^{8 \times 8}$ as

$$\begin{bmatrix} e(k) \\ u(k) \end{bmatrix}^\top \bar{P} \begin{bmatrix} e(k) \\ u(k) \end{bmatrix} \leq 1, \quad (37)$$

written in block matrix form, with blocks $P_1 \in \mathbb{R}^{6 \times 6}$, $P_2 \in \mathbb{R}^{2 \times 2}$ and $P_{12} \in \mathbb{R}^{6 \times 2}$, gives

$$\begin{bmatrix} e(k) \\ u(k) \end{bmatrix}^\top \begin{bmatrix} P_1 & P_{12} \\ P_{12}^\top & P_2 \end{bmatrix} \begin{bmatrix} e(k) \\ u(k) \end{bmatrix} \leq 1. \quad (38)$$

Which is further rewritten as

$$u(k)^\top P_2 u(k) + 2u(k)^\top P_{12}^\top e(k) + e(k)^\top P_1 e(k) \leq 1 \quad (39)$$

From (39) scaled and translated ellipsoid $u(k)^\top P_2 u(k) \leq 1$ is obtained as

$$(u(k) - a)^\top P_2 (u(k) - a) \leq \gamma, \quad (40)$$

where

$$a = -P_2^{-1} P_{12} e(k), \quad (41)$$

$$\gamma = 1 + e(k)^\top (P_{12}^\top (P_2^{-1})^\top P_{12} - P_1) e(k). \quad (42)$$

This implies the set $\mathcal{U}_k(e(k))$ defined in (35) is written equivalently as

$$\mathcal{U}_k(e(k)) = \{u(k) \mid (u(k) - a)^\top P_2 (u(k) - a) \leq \gamma\}. \quad (43)$$

To solve the problem (34) the modified fast gradient algorithm stated in Algorithm 3 can now be employed.

Algorithm 3: Set-based fast gradient method for constrained minimization

Data: Initial point $u_0 \in \mathcal{U}_{\mathcal{N}}$, $y_0 = u_0$, number of iterations i_{max} , Lipschitz constant L , scaling factors $\beta_0, \dots, \beta_{i_{\text{max}}-1}$

Calculate parameters a and γ for set $\mathcal{U}_k(e(k))$;

for $i = 0 \rightarrow i_{\text{max}} - 1$ **do**

$$v_{i+1} = y_i - \frac{1}{L} \nabla J_{\mathcal{N}}(y_i) = M y_i + g; \quad (44)$$

$$u_{i+1} = \mathbf{Proj}_{\mathcal{U}_k(x(k))}(v_{i+1}); \quad (45)$$

$$y_{i+1} = u_{i+1} + \beta_i (u_{i+1} - u_i); \quad (46)$$

end

Result: $u_{i_{\text{max}}}$

The given algorithm, in each of its iterations, finds a candidate solution v_{i+1} by making one gradient descent step using (44); if needed, the candidate solution is projected to the input constraints set $\mathcal{U}_k(e(k))$ with (45) to obtain a feasible solution u_{i+1} ; and finally using Equation (46), a scaling factor β_i is applied to obtain a better initial value for the next iteration of the algorithm.

The projection operation in Equation (45) is defined as

$$\begin{aligned} u_{i+1} &= \mathbf{Proj}_{\mathcal{U}_k(x(k))}(v_{i+1}) \\ &= \begin{cases} v_{i+1}, & \|v_{i+1} - a\|_{P_2} \leq \gamma, \\ \frac{v_{i+1} - a}{\|v_{i+1} - a\|_{P_2}} \cdot \gamma + a, & \|v_{i+1} - a\|_{P_2} > \gamma, \end{cases} \end{aligned} \quad (47)$$

where the norm $\|\cdot\|_{P_2}$ is defined as

$$\|x\|_{P_2} = \sqrt{x^\top P_2 x}. \quad (48)$$

5. Control under variable grid inductance

As an extension of the presented Set-based MPC algorithm, in this section, the grid inductance is allowed to vary over time. The grid-side inductance L_2 is modelled as

$$L_2 = L_f + L_g \quad (49)$$

where L_f represents the LCL filter inductance and L_g the possibly varying grid inductance. To model the uncertainty in the grid inductance, assume the quantity L_g

to be bounded, i.e. contained in an interval $[0, L_{\max}]$; obviously, the parameter L_2 is then constrained in

$$L_f \leq L_2 \leq L_f + L_{\max}. \quad (50)$$

Setting $\theta = \frac{1}{L_2}$, $\theta_{\min} = \frac{1}{L_f + L_{\max}}$ and $\theta_{\max} = \frac{1}{L_f}$, the parameter θ can be expressed as a convex combination of parameters θ_{\min} and θ_{\max}

$$\theta = \alpha_1 \theta_{\max} + \alpha_2 \theta_{\min}, \quad (51)$$

with $0 \leq \alpha_1, \alpha_2 \leq 1$ and $\alpha_1 + \alpha_2 = 1$. This enables us to write the system model (3), with respect to this uncertainty, as a polytopic LPV model [15]. The polytopic model consists of two vertices $(A_{c,i}, B_{c,i}, D_{c,i}, C_{c,i})$, $i \in \{1, 2\}$ that represent two possible extremes of parameter L_2 and define a polytopic matrix family in which system matrices for every permissible value of L_2 are obtained as a convex combination of the vertices, i.e.

$$A(\alpha) = \alpha_1 A_{c,1} + \alpha_2 A_{c,2}, \quad (52)$$

$$B(\alpha) = \alpha_1 B_{c,1} + \alpha_2 B_{c,2}, \quad (53)$$

$$D(\alpha) = \alpha_1 D_{c,1} + \alpha_2 D_{c,2}, \quad (54)$$

$$C(\alpha) = \alpha_1 C_{c,1} + \alpha_2 C_{c,2}, \quad (55)$$

finally the system can be written as

$$\begin{aligned} \dot{x}(t) &= A_c(\alpha(t))x(t) + B_c(\alpha(t))u(t) + D_c(\alpha(t))v(t) \\ y(t) &= C_c(\alpha(t))x(t) \end{aligned} \quad (56)$$

where $\alpha : \mathbb{R}_0^+ \rightarrow \mathbb{R}^2$ is a function of time that for every $t \geq 0$ provides scalars α_1 and α_2 . (For clarity, argument t of a function α is omitted in the rest of the paper.) Similarly to procedure in Section 2, system (56) is written in discrete time as

$$\begin{aligned} x(k+1) &= A_d(\alpha)x(k) + B_d(\alpha)u(k) + D_d(\alpha)v(k) \\ y(k) &= C_d(\alpha)x(k). \end{aligned} \quad (57)$$

Assuming the uncertain system parameter L_g is known at every time instance (i.e., is estimated) for a given reference vector $r = [i_{dr} \ i_{qr}]^\top$ the equilibrium point $[x_d \ u_d]^\top$ of a system (56) is

$$\begin{bmatrix} x_d \\ u_d \end{bmatrix} = \begin{bmatrix} A(\alpha) & B(\alpha) \\ C(\alpha) & 0 \end{bmatrix}^{-1} \begin{bmatrix} -D(\alpha)v \\ r \end{bmatrix}. \quad (58)$$

The error dynamics of a system (57) are also written as a polytopic LPV model

$$e(k+1) = A_d(\alpha)e(k) + B_d(\alpha)u_{\text{err}}(k), \quad (59)$$

where $e(k) = x(k) - x_d$, $u(k)_{\text{err}} = u(k) - u_d$ and

$$A_d(\alpha) = \alpha_1 A_{d,1} + \alpha_2 A_{d,2} \quad (60)$$

$$B_d(\alpha) = \alpha_1 B_{d,1} + \alpha_2 B_{d,2}, \quad (61)$$

for $\alpha_1, \alpha_2 \in [0, 1]$ and $\alpha_1 + \alpha_2 = 1$.

To obtain a robust stabilizing control law K , i.e., one that stabilizes the system (57) for every value of α , LMI feasibility problem (12) is extended as

$$\begin{bmatrix} P + P^T - S_i & * & * \\ \frac{1}{r}(A_{d,i} - dI)P + \frac{1}{r}B_{d,i}R & S_j & * \\ C_{d,i}P & 0 & \mu I \end{bmatrix} > 0 \quad (62)$$

for $i \in \{1, 2\}$ and $j \in \{1, 2\}$, effectively constraining the closed-loop system behavior in its two extreme vertices (with $*$ denoting appropriate transposed blocks of blocks under the main diagonal).

For calculating the sequence of robust one-step controllable ellipsoidal sets $\{\mathcal{E}_n\}_n$ that guarantee the existence of control input for every value of α and lead the system to the next ellipsoid, it is sufficient to compute the inner ellipsoidal approximation of a pre-set obtained at the system's vertices

$$\begin{aligned} \Omega(\mathcal{E}_{n-1}) &= \{x \in \mathcal{X} \mid \exists u \in \mathcal{U}, A_i x \\ &\quad + B_i u \in \mathcal{E}_{n-1}, i \in \{1, 2\}\} \\ &\supseteq \mathbf{Proj}_x \left(\mathbf{In} \left(\tilde{\mathcal{E}}_{n-1}^1 \cap \tilde{\mathcal{E}}_{n-1}^2 \cap (\mathbb{R}^6 \times \mathcal{E}^{\mathcal{U}}) \right) \right) \\ &= \mathcal{E}_n, \end{aligned} \quad (63)$$

where $\tilde{\mathcal{E}}_{n-1}^i$ is calculated using Equation (20) at both system vertices.

Based on the robust ellipsoid sequence $\{\mathcal{E}_n\}_{n \in \mathbb{N}}$, the evaluation of a set $\mathcal{U}_k(e(k))$ needed for solving the optimization problem (34) is done analogously to the procedure described in Section 4 after changing Equation (36) to

$$\bar{\mathcal{E}}_n = \mathbf{In} \left(\tilde{\mathcal{E}}_n^1 \cap \tilde{\mathcal{E}}_n^2 \cap (\mathbb{R}^6 \times \mathcal{E}^{\mathcal{U}}) \right). \quad (64)$$

6. Set-based MPC for embedded platforms

In this section, Algorithm 1 is prepared for implementation and synthesis on a microcontroller and an FPGA by precomputing all the necessary data required by the algorithm and by exploiting its structure to further ease the computational burden. Steps of the algorithm are shown in Figure 2.

Based on the procedure outlined in Section 3, the matrices P_n , for $n = 0, \dots, n_{\max}$ representing the ellipsoidal sets \mathcal{E}_n , are computed. To check whether the error state vector e is contained in an ellipsoid \mathcal{E}_n quadratic form, $e^\top P_n e$ needs to be evaluated; this operation, in m -dimensional state space consists of $(m+1)m$ multiplications and $(m+1)(m-1)$ adding operations. Because matrices P_n are positive-definite, they admit the Cholesky factorization, i.e.,

$$P_n = R_n^\top R_n \quad (65)$$

where R_n are right triangle matrices. Now the quadratic form

$$e^\top P_n e = e^\top R_n^\top R_n e = (R_n e)^\top (R_n e) \quad (66)$$

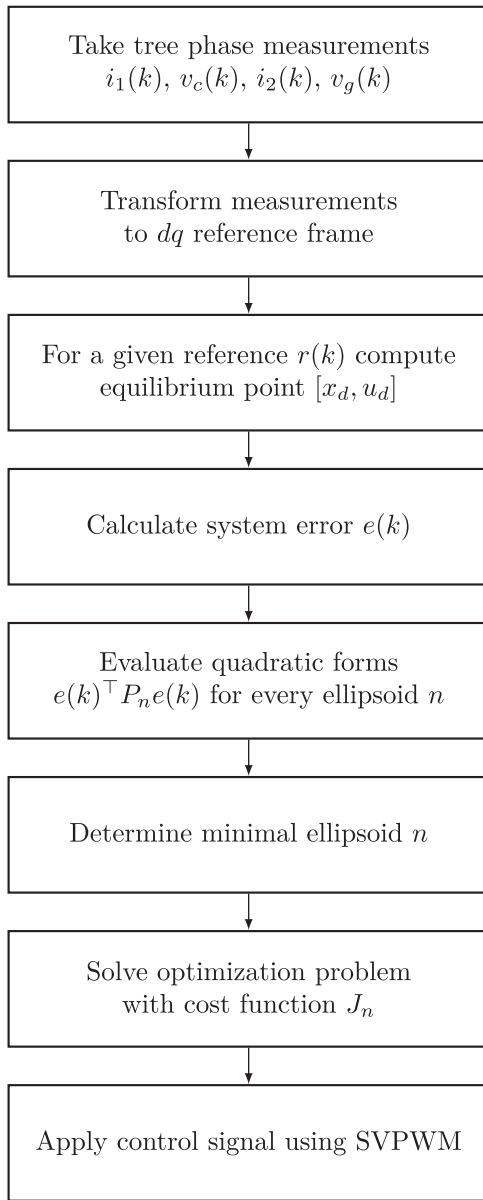


Figure 2. Flow chart of the Set-based MPC algorithm.

can be evaluated with $\frac{1}{2}m(m+3)$ multiplications and $\frac{1}{2}(m+2)(m-1)$ additions.

To find the index of a minimal ellipsoid, a simple parallel reduction procedure is done for all the indexes satisfying

$$e^T P_n e \leq 1 \quad (67)$$

that finds the minimum with $m-1$ comparison operations in $\log_2 m$ “steps”.

Based on the found ellipsoid index n , the fast gradient method is used to solve the MPC optimization problem with an appropriate cost function

$$J_n(u) = (Ae + Bu)^T P_{n-1} (Ae + Bu), \quad (68)$$

the gradient of which is

$$\nabla J_i(u) = 2B^T P_{n-1} Bu + 2B^T P_{n-1} Ae. \quad (69)$$

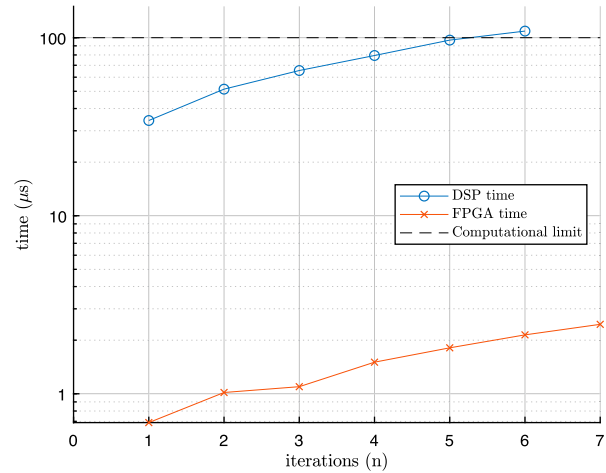


Figure 3. Comparison of computational times between DSP and FPGA implementations for different values of maximum number of iterations.

Now the gradient step in Algorithm 3 can be computed as

$$v_{i+1} = My_i + g, \quad (70)$$

with

$$M = I - \frac{2}{L} B^T P_{n-1} B \quad (71)$$

and

$$g = -\frac{2}{L} B^T P_{n-1} Ae =: He, \quad (72)$$

where M and H are computed offline. Similarly, the matrices used in the projection step of the algorithm are precomputed using formulas (41) and (42).

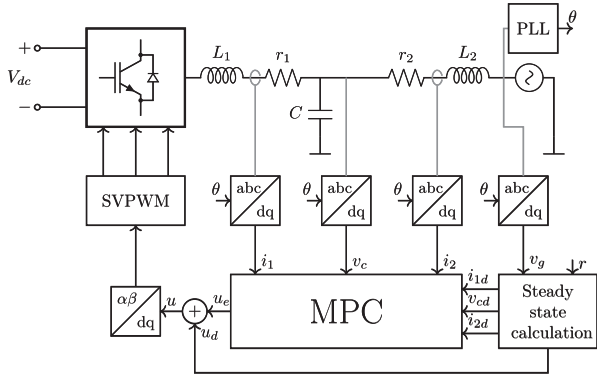
7. Results

To check the real-time computation ability of the proposed controller, Algorithm 3 is first implemented on Texas Instruments TMS320F28335 DSP and a Xilinx Artix-7 XC7A200T FPGA device. Although the FGM, due to the projection step, guarantees feasibility at any number of iterations, the quality of the solution (in terms of steady-state error, harmonic distortion, etc.) increases with the number of iterations taken. The computational times were recorded depending on the number of iteration steps in FGM algorithm. The computational limit is set at 100 μs , which corresponds to the switching time of SVPWM. As can be seen in Figure 3, execution time depends on the maximum number of FGM iterations, with Texas Instruments DSP reaching the limit for five maximum iterations, while Xilinx FPGA shows promising results with 7 steps taking less than 3 μs .

Table 1 shows the FPGA resources utilized to implement the proposed controller, proving the design viable on a commercial FPGA device.

Table 1. FPGA resources occupied by FGM depending on the number of iterations i_{\max} .

i_{\max}	LUT (% of 133 800)	DSP blocks (% of 740)
1	60 508 (44%)	363(49%)
2	65 135 (48%)	393(53%)
3	70 349 (52%)	423(57%)
4	75 155 (55%)	453(61%)
5	79 995 (59%)	483(65%)
6	84 834 (63%)	513(69%)
7	89 669 (66%)	543(73%)

**Figure 4.** Simulation diagram of the grid-tied power converter.

The dynamical response of a system controlled with the proposed algorithm was tested in simulation. MATLAB/Simulink was used for the simulation of the power converter, LCL filter, and grid, while the control algorithm was implemented on an FPGA device, as shown in Figure 4 (the communication between MATLAB and the FPGA board was realized using a JTAG connection).

For the grid-tied power converter with an LCL filter and parameters given in Table 2 and zero grid inductance (nominal case), the state feedback controller K_{nominal} is synthesized by solving the problem (12). From the computed gain

$$K_{\text{nominal}}^T = \begin{bmatrix} 49.0670 & -1.0850 \\ 1.0850 & 49.0670 \\ 44.8137 & -2.2063 \\ 2.2063 & 44.8137 \\ 20.3838 & -3.8242 \\ 3.8242 & 20.3838 \end{bmatrix}, \quad (73)$$

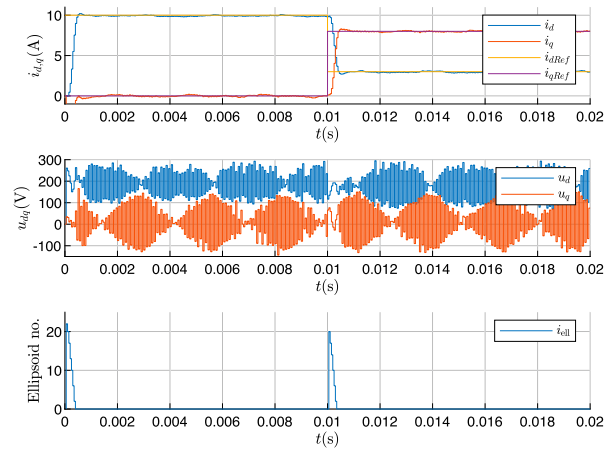
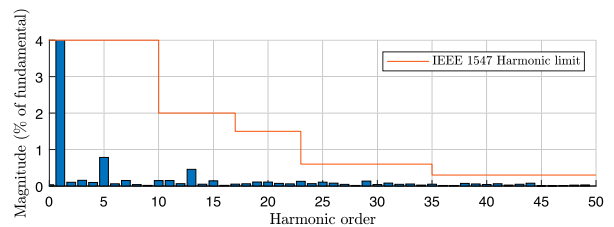
an invariant ellipsoidal set, and a family of one-step controllable ellipsoidal sets are computed by solving optimization problem (28). The objective functions defined as

$$J(u_{\text{err}})(k)_{n(k)} = \|(A_d e(k) + B_d u_{\text{err}}(k))\|_{P_{n(k)-1}} \quad (74)$$

where $P_{n(k)-1}$ is a matrix representing $n(k) - 1$ ellipsoid, are chosen to provide a minimum time control. Based on the objective function $J_n(k)$, the Lipschitz constant L , scaling factors $\beta_0, \dots, \beta_{i_{\max}-1}$, and matrices M and H , used in Algorithm 3, are computed offline as described in Section 6 and used as constants in the FPGA implementation.

Table 2. Inverter and grid parameters.

Symbol	Description	Value	Unit
r_1	Inverter resistance	0.5	Ω
L_1	Filter inductance	1	mH
C	Filter capacitance	62	μF
r_2	Grid resistance	0.5	Ω
L_f	Filter inductance	0.3	mH
L_g	Grid inductance variation	0–1	mH
V_{dc}	DC link voltage	420	V
v_g	Grid peak voltage	180	V
f	Grid frequency	60	Hz
f_{PWM}	PWM frequency	10	kHz
f_s	Sampling frequency	20	kHz

**Figure 5.** Simulation results: reference tracking for the nominal system (top), control signal (middle), index of an ellipsoid containing the current system state (bottom).**Figure 6.** Harmonic content of the phase a injected current i_a nominal system, THD = 1.11%.

The reference tracking capabilities of a proposed controller were tested in simulation; as observed in Figure 5, the reference was set to $i_d = 10\text{A}$, $i_q = 0\text{A}$ at time $t = 0\text{s}$, and changed to $i_d = 3\text{A}$, $i_q = 8\text{A}$ at $t = 0.01\text{s}$. The system shows fast dynamic response and accurate tracking capabilities while satisfying the input and state constraints. As the quality of grid-injected current is of concern, an FFT analysis of the phase a grid current was conducted. As shown in Figure 6, the injected current satisfies the IEEE 1547 norm constraints on per-harmonic content and with a THD of 1.11%, satisfies the standard's required limit of 5%.

For the case of the grid-tied power converter with an LCL filter and variable grid inductance in the range 0–1 mH (robust case), the robust state feedback

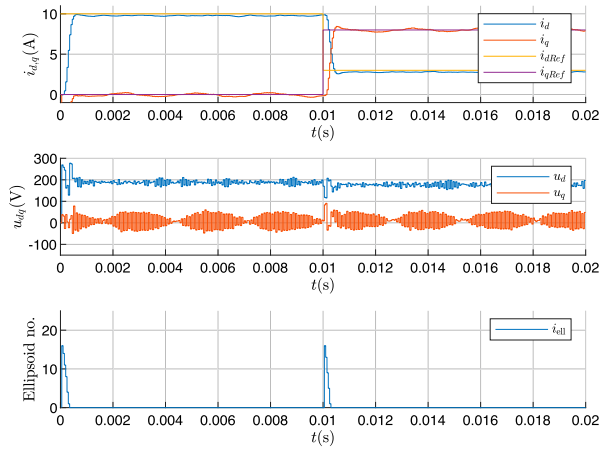


Figure 7. Simulation results: reference tracking for LPV modelled system in vertex with $L_g = 0$ mH (top), control signal (middle), index of an ellipsoid containing the current system state (bottom).

controller K_{robust} is synthesized by solving the problem (62). From the computed gain

$$K_{\text{robust}}^{\top} = \begin{bmatrix} 34.6422 & -1.3389 \\ 1.3389 & 34.6422 \\ 21.7514 & -1.9158 \\ 1.9158 & 21.7514 \\ 8.3042 & -3.5936 \\ 3.5936 & 8.3042 \end{bmatrix}, \quad (75)$$

robust invariant ellipsoidal set, and a family of robust one-step controllable ellipsoidal sets are computed. The parameter-dependent objective functions are defined as

$$J(u_{\text{err}}(k); \alpha)_{n(k)} = \|A_d(\alpha)e(k) + B_d(\alpha)u_{\text{err}}(k)\|_{P_{n(k)-1}}, \quad (76)$$

where parameter α representing the change of grid inductance, is estimated online.

The simulation conducted for the nominal case is here repeated for two extreme cases of grid inductance, i.e., $L_g = 0$ mH and $L_g = 1$ mH. As seen in Figure 7, the dynamic response for the first case is similar to the nominal case, but with higher harmonic content as seen in Figure 8 and a higher THD of 1.78% than the nominal case. In the second case, the system shows a slower dynamic response owing to high grid inductance (Figure 9) but a lower THD of 1.19% (Figure 10). The simulations confirm the system's stability, good reference tracking, and high quality of the injected current regardless of the uncertainty in the grid inductance.

8. Conclusion

In this paper, a computationally efficient MPC algorithm for grid-tied power converters is proposed by modifying the fast gradient projection method using invariant set theory. The proposed algorithm was implemented and tested through hardware-in-the-loop

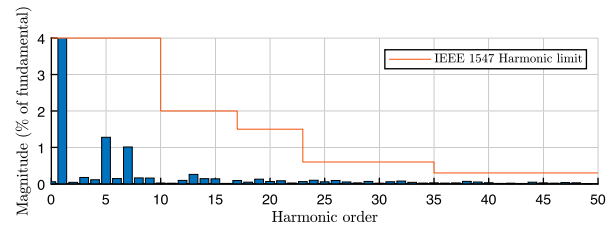


Figure 8. Harmonic content of the phase a injected current i_a for LPV modelled system in vertex with $L_g = 0$ mH, THD = 1.78%.

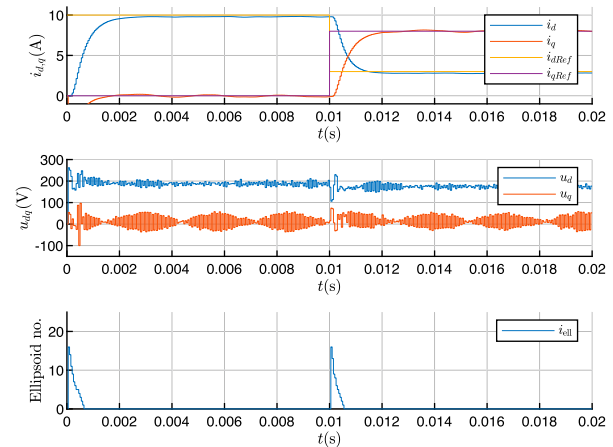


Figure 9. Simulation results: reference tracking for LPV modelled system in vertex with $L_g = 1$ mH (top), control signal (middle), index of an ellipsoid containing the current system state (bottom).

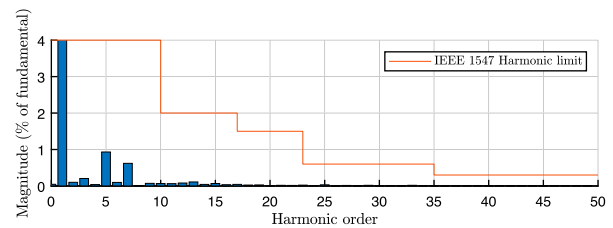


Figure 10. Harmonic content of the phase a injected current i_a for LPV modelled system in vertex with $L_g = 1$ mH, THD = 1.19%.

simulation using Texas Instruments DSP and Xilinx FPGA platforms, showing execution times that satisfy timing constraints for real-time execution. Furthermore, the MPC algorithm is shown to be easily extended to include uncertainties in grid inductance while maintaining good dynamic response in reference tracking and low current THD.

Disclosure statement

No potential conflict of interest was reported by the author(s).

ORCID

Jadranko Matuško  <http://orcid.org/0000-0002-7259-0957>

References

- [1] Kouro S, Perez MA, Rodriguez J, et al. Model predictive control: MPC's role in the evolution of power electronics. *IEEE Ind Electron Mag.* 2015;9(4):8–21.
- [2] Vazquez S, Rodriguez J, Rivera M, et al. Model predictive control for power converters and drives: advances and trends. *IEEE Trans Ind Electron.* 2016;64(2):935–947.
- [3] Karamanakos P, Liegmann E, Geyer T, et al. Model predictive control of power electronic systems: methods, results, and challenges. *IEEE Open J Ind Appl.* 2020;1:95–114.
- [4] Aguilera RP, Quevedo DE. Predictive control of power converters: designs with guaranteed performance. *IEEE Trans Ind Inform.* 2014;11(1):53–63.
- [5] Preindl M. Robust control invariant sets and Lyapunov-based MPC for IPM synchronous motor drives. *IEEE Trans Ind Electron.* 2016;63(6):3925–3933.
- [6] Young HA, Perez MA, Rodriguez J, et al. Assessing finite-control-set model predictive control: a comparison with a linear current controller in two-level voltage source inverters. *IEEE Ind Electron Mag.* 2014;8(1):44–52.
- [7] Geyer T, Quevedo DE. Multistep finite control set model predictive control for power electronics. *IEEE Trans Power Electron.* 2014;29(12):6836–6846.
- [8] Falkowski P, Sikorski A. Finite control set model predictive control for grid-connected ac–dc converters with LCL filter. *IEEE Trans Ind Electron.* 2017;65(4):2844–2852.
- [9] Preindl M, Bolognani S. Comparison of direct and PWM model predictive control for power electronic and drive systems. In: 2013 Twenty-Eighth Annual IEEE Applied Power Electronics Conference and Exposition (APEC). IEEE; 2013, p. 2526–2533.
- [10] Reznik A, Simoes MG, Al-Durra A, et al. Lcl filter design and performance analysis for grid-interconnected systems. *IEEE Trans Ind Appl.* 2013;50(2):1225–1232.
- [11] Richter S, Mariethoz S, Morari M. High-speed online MPC based on a fast gradient method applied to power converter control. In: Proceedings of the 2010 American Control Conference. IEEE; 2010. p. 4737–4743.
- [12] Preindl M, Bolognani S, Danielson C. Model predictive torque control with PWM using fast gradient method. In: 2013 Twenty-Eighth Annual IEEE Applied Power Electronics Conference and Exposition (APEC). IEEE; 2013. p. 2590–2597.
- [13] Ma Z, Saeidi S, Kennel R. FPGA implementation of model predictive control with constant switching frequency for PMSM drives. *IEEE Trans Ind Inform.* 2014;10(4):2055–2063.
- [14] Angeli D, Casavola A, Franzè G, et al. An ellipsoidal offline MPC scheme for uncertain polytopic discrete-time systems. *Automatica.* 2008;44(12):3113–3119.
- [15] Boyd S, El Ghaoui L, Feron E, et al. *Linear matrix inequalities in system and control theory.* Vol. 15. SIAM; 1994.
- [16] Maccari L, Massing J, Schuch L, et al. Robust h_∞ control for grid connected PWM inverters with LCL filters. In: 2012 10th IEEE/IAS International Conference on Industry Applications. IEEE; 2012. p. 1–6.